

STUDIES ON SYNTHESIS AND MAGNETIC PROPERTY OF $\text{Ln}_x\text{Eu}_{1-x}\text{CoO}_3$ ($\text{Ln}=\text{Gd}, \text{Ho}; x=0\sim 1$) PREPARED BY MEANS OF THERMAL DECOMPOSITION OF $\text{Ln}_x\text{Eu}_{1-x}[\text{Co}(\text{CN})_6]\cdot n\text{H}_2\text{O}$ ($\text{Ln}=\text{Gd}, \text{Ho}; x=0\sim 1$)

R. Sawano¹ and Y. Masuda^{2*}

¹Graduate School of Science and Technology, Niigata University 2-8050 Ikarashi, Niigata 950-2181, Japan

²Department of Environmental Science, Faculty of Science, Niigata University, 2-8050 Ikarashi, Niigata 950-2181, Japan

The perovskite-type oxides, $\text{Gd}_x\text{Eu}_{1-x}\text{CoO}_3$ and $\text{Ho}_x\text{Eu}_{1-x}\text{CoO}_3$ were prepared by the thermal decompositions $\text{Gd}_x\text{Eu}_{1-x}[\text{Co}(\text{CN})_6]\cdot 4\text{H}_2\text{O}$ and $\text{Ho}_x\text{Eu}_{1-x}[\text{Co}(\text{CN})_6]\cdot 4\text{H}_2\text{O}$, respectively. $\text{Gd}_x\text{Eu}_{1-x}\text{CoO}_3$ and $\text{Ho}_x\text{Eu}_{1-x}\text{CoO}_3$ were orthorhombic and Pnma. In the ranges of $0 \leq x \leq 1$, their lattice parameters of a -axis linearly lengthen with the increase of the value of x , but those of b and c axes decrease with the increase of x .

The magnetic susceptibility of EuCoO_3 showed a typical Van Vleck paramagnetic property. The Co^{3+} ions in EuCoO_3 were in the low spin state ($t_{2g}^6 e_g^0, S=0$), therefore the susceptibility of EuCoO_3 was dependent on the Eu^{3+} ions in the temperature range from 5 to 300 K. Similarly, the Co^{3+} ions in $\text{Gd}_x\text{Eu}_{1-x}\text{CoO}_3$ and $\text{Ho}_x\text{Eu}_{1-x}\text{CoO}_3$ were also in the low spin state ($t_{2g}^6 e_g^0, S=0$), therefore the susceptibilities of $\text{Gd}_x\text{Eu}_{1-x}\text{CoO}_3$ and $\text{Ho}_x\text{Eu}_{1-x}\text{CoO}_3$ were dependent on the component of the Eu^{3+} , Gd^{3+} and Ho^{3+} ions in the temperature ranges from 5 to 300 K.

Keywords: $\text{Gd}_x\text{Eu}_{1-x}\text{CoO}_3$, $\text{Ho}_x\text{Eu}_{1-x}\text{CoO}_3$, magnetic susceptibilities of perovskite-type oxides, perovskite-type oxides, prepared of perovskite-type oxides by thermal decomposition

Introduction

Major synthetic method for perovskite-type oxide is the solid-state reaction method. In the method, mixture of metallic oxides is well ground, pelletized and fired. These procedures are repeated by two or three times, and the perovskite-type oxide can be obtained. But it is difficult to change stoichiometric ratio of the product metals in the method and the method requires high calcining temperature [1, 2].

Recently, perovskite-type oxides have been prepared by means of the thermal decompositions of heteronuclear complexes. In 1968, Gallagher proposed that LaFeO_3 and LaCoO_3 were prepared by use of the thermal decompositions of the appropriate hexacyanometallate complexes, as $\text{La}[\text{Fe}(\text{CN})_6]\cdot 5\text{H}_2\text{O}$ and $\text{La}[\text{Co}(\text{CN})_6]\cdot 5\text{H}_2\text{O}$, respectively [3].

The series complexes of $\text{Ln}[\text{M}(\text{CN})_6]\cdot n\text{H}_2\text{O}$ ($\text{Ln}=\text{La}\sim\text{Lu}$) are easily prepared by the reactions of $\text{K}_3[\text{M}(\text{CN})_6]$ ($\text{M}=\text{Fe, Co}$) and LnX_3 ($X=\text{Cl, NO}_3$) in aqueous solution [4, 5], and the homogeneous oxides can be obtained by means of their thermal decompositions. It is noteworthy that the decomposition provides the oxide at lower temperature than that of solid-state reaction method.

The structures, electric and magnetic properties of the perovskite-type oxides have been investigated

for a long time. For example, LaCoO_3 has two magnetic transitions at 120 and 500 K. Asai *et al.* [6] reported that the low spin ground state of Co^{3+} ($t_{2g}^6 e_g^0, S=0$) was changed to the intermediate spin state ($t_{2g}^5 e_g^1, S=1$) in the first transition and the intermediate spin state was transformed to the high spin state ($t_{2g}^4 e_g^2, S=2$) in the second transition.

Umemoto *et al.* [7] reported the structures and the magnetic properties of $\text{Ce}_x\text{Eu}_{1-x}\text{CoO}_3$ ($x=0.1$ and 0.15) prepared by means of thermal decomposition of $\text{Ce}_x\text{Eu}_{1-x}[\text{Co}(\text{CN})_6]\cdot 4\text{H}_2\text{O}$. In $\text{Ce}_x\text{Eu}_{1-x}\text{CoO}_3$, the Ce^{3+} ion is expected to oxidize more easily to Ce^{4+} ion than the other trivalent lanthanide ions, and the Eu^{2+} ion is more stable than the other divalent lanthanide ions. So they measured the magnetic susceptibilities of $\text{Ce}_x\text{Eu}_{1-x}\text{CoO}_3$, but the valence states of Ce and Eu were estimated to be trivalent as Ce^{3+} and Eu^{3+} , respectively.

Authors expect that the new properties of $\text{Ln}_x\text{Eu}_{1-x}\text{CoO}_3$ would break out by the substitution of Ln ion with the another Ln' ion which has different ionic radius of Ln ion. So in this study, Ln was substituted by Gd or Ho ion because the ionic radius of Gd ion is close to that of Eu ion and the radius of Ho^{3+} ion is smaller than that of Eu^{3+} ion. The perovskite-type oxides, $\text{Ln}_x\text{Eu}_{1-x}\text{CoO}_3$ ($\text{Ln}=\text{Gd}, \text{Ho}; x=0\sim 1$) were prepared by means of the thermal decom-

* Author for correspondence: y-mashuda@ecatv.home.ne.jp

positions of $\text{Ln}_x\text{Eu}_{1-x}[\text{Co}(\text{CN})_6]\cdot n\text{H}_2\text{O}$ ($\text{Ln}=\text{Gd}, \text{Ho}; x=0\sim 1$) and studied their structures and magnetic properties.

Experimental

Chemicals and preparations

$\text{Gd}_x\text{Eu}_{1-x}[\text{Co}(\text{CN})_6]\cdot 4\text{H}_2\text{O}$ ($x=0\sim 1$) were synthesized by the stoichiometrical mixing of the aqueous solutions of $\text{K}_3[\text{Co}(\text{CN})_6]$, $\text{EuCl}_3\cdot 8\text{H}_2\text{O}$ and $\text{Gd}(\text{NO}_3)_3\cdot 6\text{H}_2\text{O}$ at 360 K. $\text{Ho}_x\text{Eu}_{1-x}[\text{Co}(\text{CN})_6]\cdot 4\text{H}_2\text{O}$ ($x=0\sim 1$) were also synthesized by the mixing of the aqueous solutions of $\text{K}_3[\text{Co}(\text{CN})_6]$, $\text{EuCl}_3\cdot 8\text{H}_2\text{O}$ and $\text{HoCl}_3\cdot 8.5\text{H}_2\text{O}$ at 360 K.

$\text{EuCl}_3\cdot 8\text{H}_2\text{O}$ and $\text{HoCl}_3\cdot 8.5\text{H}_2\text{O}$ were obtained by the reaction of Ln_2O_3 ($\text{Ln}=\text{Eu}, \text{Ho}$) and 36 mass% HCl. Eu_2O_3 , Ho_2O_3 and $\text{Gd}(\text{NO}_3)_3\cdot 6\text{H}_2\text{O}$ were purchased from Shinetsu Chemical Co., their purities were 99.9% and used without further purification. $\text{K}_3[\text{Co}(\text{CN})_6]$ was purchased from Sigma Aldrich Co., and used after the purification by recrystallization from distilled water.

$\text{Gd}_x\text{Eu}_{1-x}\text{CoO}_3$ ($x=0\sim 1$) were prepared by heating $\text{Gd}_x\text{Eu}_{1-x}[\text{Co}(\text{CN})_6]\cdot 4\text{H}_2\text{O}$ ($x=0\sim 1$) to 1473 K for 2 h in an ADVANTEC electric furnace KT-1533. $\text{Ho}_x\text{Eu}_{1-x}\text{CoO}_3$ ($x=0\sim 1$) were also prepared by heating $\text{Ho}_x\text{Eu}_{1-x}[\text{Co}(\text{CN})_6]\cdot 4\text{H}_2\text{O}$ ($x=0\sim 1$) to 1163 K for 15 h in the electric furnace.

Methods

Thermal analyses

TG and DTA curves were simultaneously recorded on a Rigaku Thermoflex TAS 200. About 10 mg of sample was weighed into a platinum crucible and heated to 1223 K with heating rate of 10 K min⁻¹ in air atmosphere. An alumina was used as a reference.

X-ray powder diffraction (XRD)

XRD profiles of samples were obtained by means of a Rigaku Geigerflex RAD-3C diffractometer equipped with a high temperature sample holder. CuK_α radiation ($\lambda=1.5418 \text{ \AA}$) was mono-chromatized by use of a graphite monochromator. The X-ray generator was operated at the voltage of 40 kV and the current of 30 mA. The diffraction data were collected at the 2θ ranges from 10 to 70° with a step-scan width 0.02° and fixed counting (1.5 times) procedure [4, 5, 7].

The lattice parameters of $\text{Ln}_x\text{Eu}_{1-x}[\text{Co}(\text{CN})_6]\cdot 4\text{H}_2\text{O}$ ($\text{Ln}=\text{Gd}, \text{Ho}; x=0\sim 1$) and $\text{Ln}_x\text{Eu}_{1-x}\text{CoO}_3$ ($\text{Ln}=\text{Gd}, \text{Ho}; x=0\sim 1$) were determined by use of the CELL program, and the refinements of their

structures were performed by means of the Rietveld method using the RIETAN 2000 [7, 8].

Magnetic susceptibility

The magnetic susceptibilities of $\text{Gd}_x\text{Eu}_{1-x}\text{CoO}_3$ and $\text{Ho}_x\text{Eu}_{1-x}\text{CoO}_3$ were measured in a SQUID magnetometer, Quantum Design MPMS-XL in the temperature range from 5 to 300 K with an applied field at 100 Oe [7].

Result and discussion

The structures of $\text{Gd}_x\text{Eu}_{1-x}[\text{Co}(\text{CN})_6]\cdot 4\text{H}_2\text{O}$ ($x=0\sim 1$) and $\text{Ho}_x\text{Eu}_{1-x}[\text{Co}(\text{CN})_6]\cdot 4\text{H}_2\text{O}$ ($x=0\sim 1$)

The TG-DTA curves for both the complexes $\text{Gd}_{0.5}\text{Eu}_{0.5}[\text{Co}(\text{CN})_6]\cdot n\text{H}_2\text{O}$ and $\text{Ho}_{0.5}\text{Eu}_{0.5}[\text{Co}(\text{CN})_6]\cdot 4\text{H}_2\text{O}$ were shown in Fig. 1. The mass losses of $\text{Gd}_{0.5}\text{Eu}_{0.5}[\text{Co}(\text{CN})_6]\cdot n\text{H}_2\text{O}$ and $\text{Ho}_{0.5}\text{Eu}_{0.5}[\text{Co}(\text{CN})_6]\cdot n\text{H}_2\text{O}$ observed below 500 K were due to the dehydration [4, 9], and the values, 16.5 and 16.4% were close to the theoretical ones, 16.6 and 16.2% calculated for $\text{Gd}_{0.5}\text{Eu}_{0.5}[\text{Co}(\text{CN})_6]\cdot 4\text{H}_2\text{O}$ and

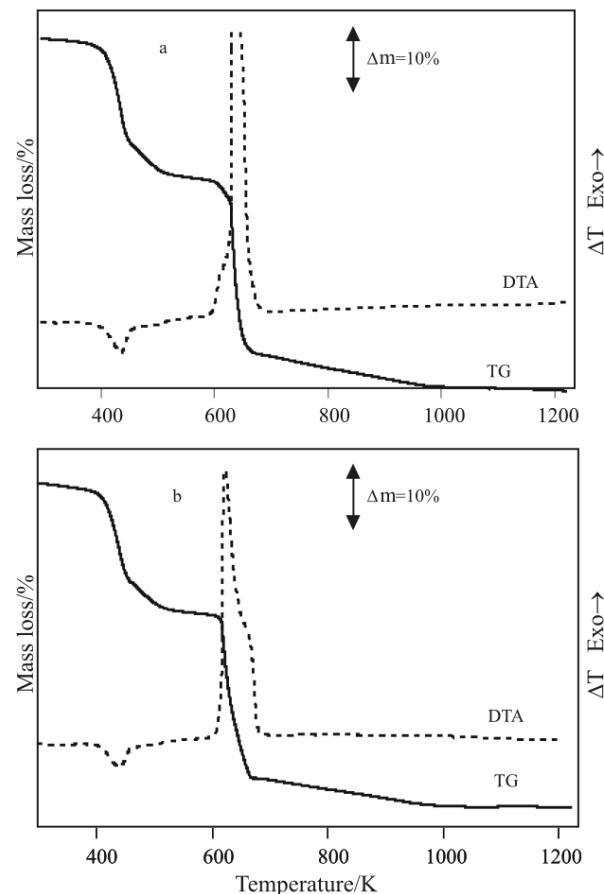


Fig. 1 TG-DTA curves of a – $\text{Gd}_{0.5}\text{Eu}_{0.5}[\text{Co}(\text{CN})_6]\cdot n\text{H}_2\text{O}$ and b – $\text{Ho}_{0.5}\text{Eu}_{0.5}[\text{Co}(\text{CN})_6]\cdot n\text{H}_2\text{O}$

$\text{Ho}_{0.5}\text{Eu}_{0.5}[\text{Co}(\text{CN})_6]\cdot 4\text{H}_2\text{O}$, respectively. Similarly, the n of the series hydrates of $\text{Gd}_x\text{Eu}_{1-x}[\text{Co}(\text{CN})_6]\cdot n\text{H}_2\text{O}$ and $\text{Ho}_x\text{Eu}_{1-x}[\text{Co}(\text{CN})_6]\cdot n\text{H}_2\text{O}$ were also estimated to be 4 from the TG-DTA.

After the dehydration, an abrupt mass loss accompanying an exotherm at around 630 K and gradual decrease were observed up to 1000 K, followed by a plateau. These decomposition profiles were similar to that of $\text{La}[\text{Co}(\text{CN})_6]\cdot 5\text{H}_2\text{O}$ [10–12].

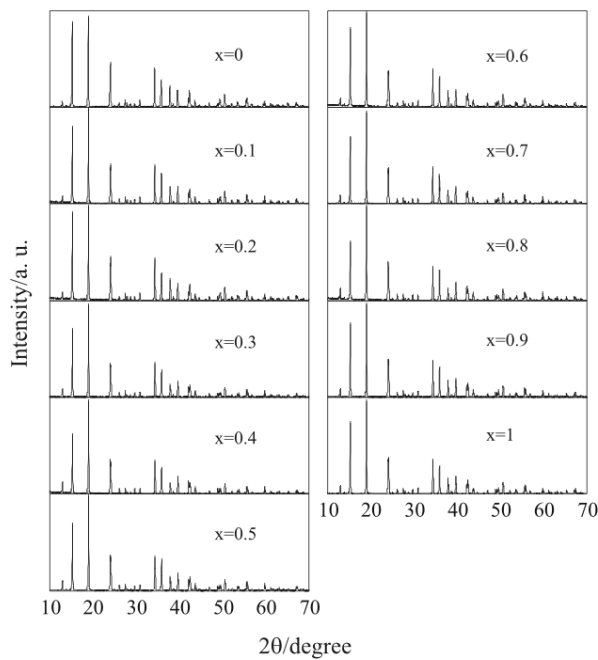


Fig. 2 XRD profiles of $\text{Gd}_x\text{Eu}_{1-x}[\text{Co}(\text{CN})_6]\cdot 4\text{H}_2\text{O}$

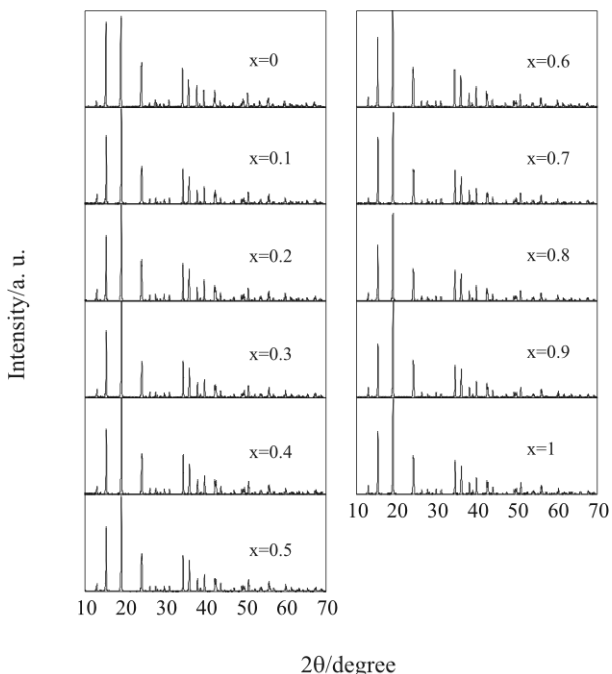


Fig. 3 XRD profiles of $\text{Ho}_x\text{Eu}_{1-x}[\text{Co}(\text{CN})_6]\cdot 4\text{H}_2\text{O}$

The abrupt mass loss seems to be attributed to the cleavage and combustion of CN group, and the gradual decrease to be mainly correspond to the evolution of carbon dioxide. At around 1000 K, the perovskite-type oxide was obtained.

Figures 2 and 3 show the XRD profiles of $\text{Gd}_x\text{Eu}_{1-x}[\text{Co}(\text{CN})_6]\cdot 4\text{H}_2\text{O}$ and $\text{Ho}_x\text{Eu}_{1-x}[\text{Co}(\text{CN})_6]\cdot 4\text{H}_2\text{O}$, respectively. The crystal structure of $\text{Eu}[\text{Co}(\text{CN})_6]\cdot 4\text{H}_2\text{O}$ is known to be orthorhombic and $Cmcm$ [13]. Both the structures of the series complexes of $\text{Gd}_x\text{Eu}_{1-x}[\text{Co}(\text{CN})_6]\cdot 4\text{H}_2\text{O}$ and $\text{Ho}_x\text{Eu}_{1-x}[\text{Co}(\text{CN})_6]\cdot 4\text{H}_2\text{O}$ were also assumed to be orthorhombic and $Cmcm$, because their XRD profiles were similar to that of $\text{Eu}[\text{Co}(\text{CN})_6]\cdot 4\text{H}_2\text{O}$.

The X-ray diffraction peaks of $\text{Gd}_x\text{Eu}_{1-x}[\text{Co}(\text{CN})_6]\cdot 4\text{H}_2\text{O}$ and $\text{Ho}_x\text{Eu}_{1-x}[\text{Co}(\text{CN})_6]\cdot 4\text{H}_2\text{O}$ shifted into higher angles with increase of the value of x . Their lattice parameters predicted by use of the CELL program were refined by means of the Rietveld method using the RIETAN 2000. The lattice parameters linearly decreased with the increase of the value of x (Figs 4 and 5), however remarkable changes correlated to the change of x were not observed for the thermal dehydrations and decompositions of $\text{Gd}_x\text{Eu}_{1-x}[\text{Co}(\text{CN})_6]\cdot 4\text{H}_2\text{O}$ and $\text{Ho}_x\text{Eu}_{1-x}[\text{Co}(\text{CN})_6]\cdot 4\text{H}_2\text{O}$.

The structures of $\text{Gd}_x\text{Eu}_{1-x}\text{CoO}_3$ ($x=0\sim 1$) and $\text{Ho}_x\text{Eu}_{1-x}\text{CoO}_3$ ($x=0\sim 1$)

Figures 6 and 7 show the XRD profiles of the residues obtained by heating $\text{Gd}_x\text{Eu}_{1-x}[\text{Co}(\text{CN})_6]\cdot 4\text{H}_2\text{O}$ to 1473 K and those of heating $\text{Ho}_x\text{Eu}_{1-x}[\text{Co}(\text{CN})_6]\cdot 4\text{H}_2\text{O}$ to 1163 K, respectively. The final product of

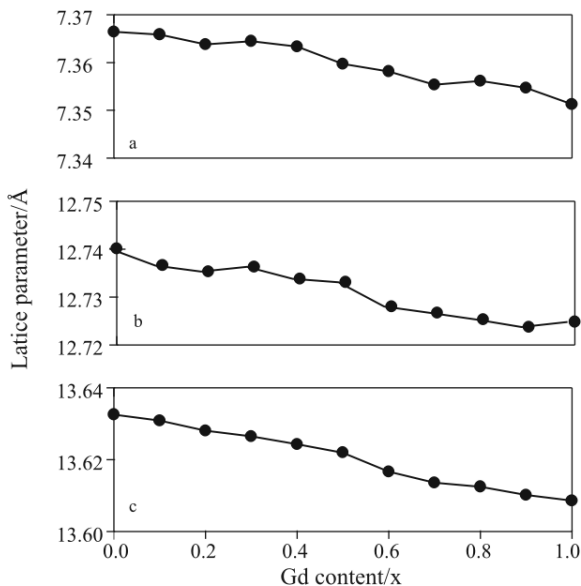


Fig. 4 Relationships between lattice parameters and contents of Gd, x of $\text{Gd}_x\text{Eu}_{1-x}[\text{Co}(\text{CN})_6]\cdot 4\text{H}_2\text{O}$; a – a -axis, b – b -axis and c – c -axis

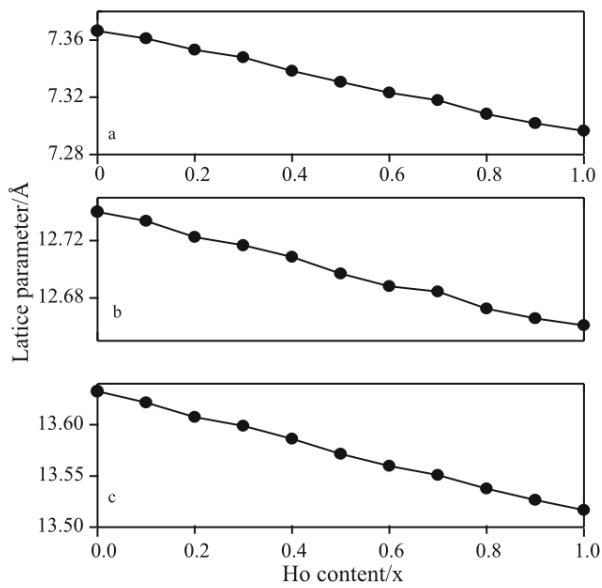


Fig. 5 Relationships between lattice parameters and contents of Ho, x of $\text{Ho}_x\text{Eu}_{1-x}[\text{Co}(\text{CN})_6]\cdot 4\text{H}_2\text{O}$; a – a -axis, b – b -axis and c – c -axis

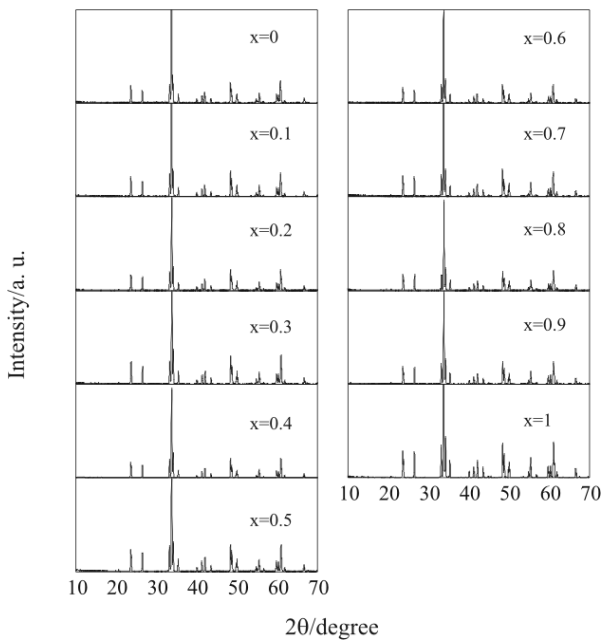


Fig. 6 XRD profiles of residues of $\text{Gd}_x\text{Eu}_{1-x}[\text{Co}(\text{CN})_6]\cdot 4\text{H}_2\text{O}$ heated to 1473 K

the thermal decomposition of $\text{Eu}[\text{Co}(\text{CN})_6]\cdot 4\text{H}_2\text{O}$ is known to be EuCoO_3 [7, 14]. The profiles of the final residues of $\text{Gd}_x\text{Eu}_{1-x}[\text{Co}(\text{CN})_6]\cdot 4\text{H}_2\text{O}$ and $\text{Ho}_x\text{Eu}_{1-x}[\text{Co}(\text{CN})_6]\cdot 4\text{H}_2\text{O}$ were similar to that of EuCoO_3 .

The lattice parameters of these oxides predicted by use of the CELL program were refined by means of the Rietveld method using the RIETAN 2000. The lattice parameter of a -axis linearly lengthens with

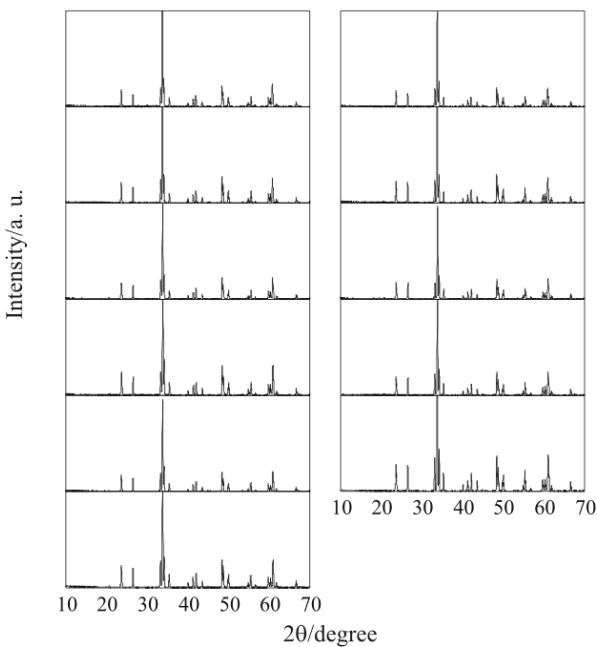


Fig. 7 XRD profiles of residues of $\text{Ho}_x\text{Eu}_{1-x}[\text{Co}(\text{CN})_6]\cdot 4\text{H}_2\text{O}$ heated to 1163 K

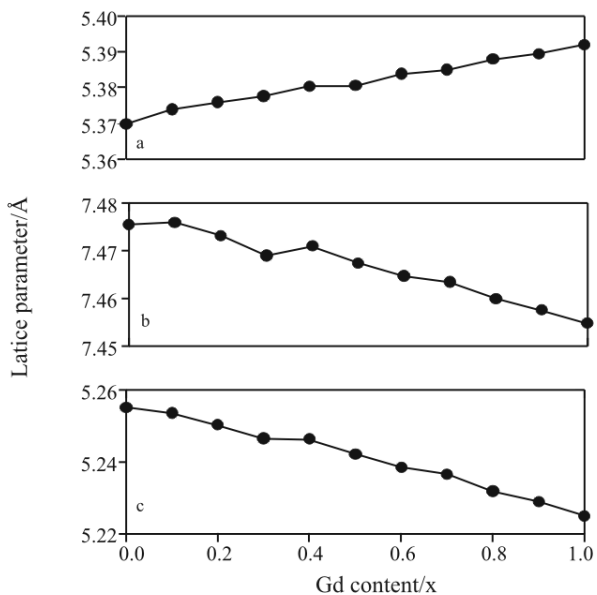


Fig. 8 Relationships between lattice parameters and contents of Gd, x of $\text{Gd}_x\text{Eu}_{1-x}\text{CoO}_3$; a – a -axis, b – b -axis and c – c -axis

the increase of the value of x , but those of b - and c -axes decreased with the increase of the value of x (Figs 8 and 9). These results were indicated that Eu atoms of EuCoO_3 were replaced smoothly with Gd and Ho atoms in the ranges of $0 \leq x \leq 1$.

The profiles observed for $\text{Gd}_{0.5}\text{Eu}_{0.5}\text{CoO}_3$ and $\text{Ho}_{0.5}\text{Eu}_{0.5}\text{CoO}_3$ were in good agreement with the calculated ones (Fig. 10). The reliability factors and the ‘Goodness-of-fit’ indicator, S for both the oxides are shown in Table 1. From these results, both the

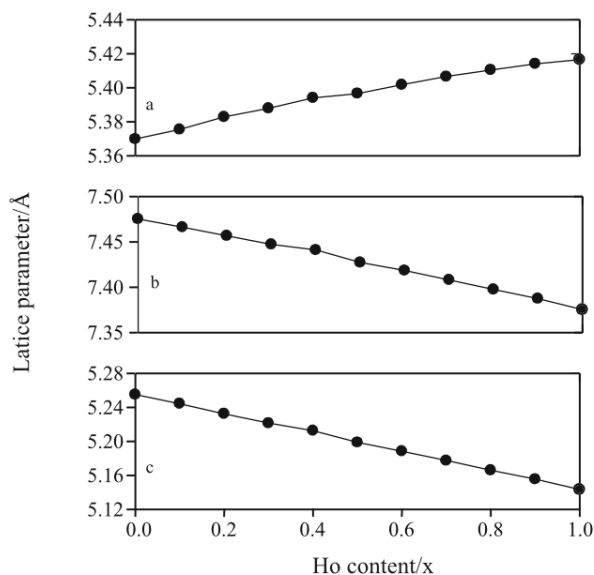


Fig. 9 Relationships between lattice parameters and contents of Ho, x of $\text{Ho}_x\text{Eu}_{1-x}\text{CoO}_3$; a – a -axis, b – b -axis and c – c -axis

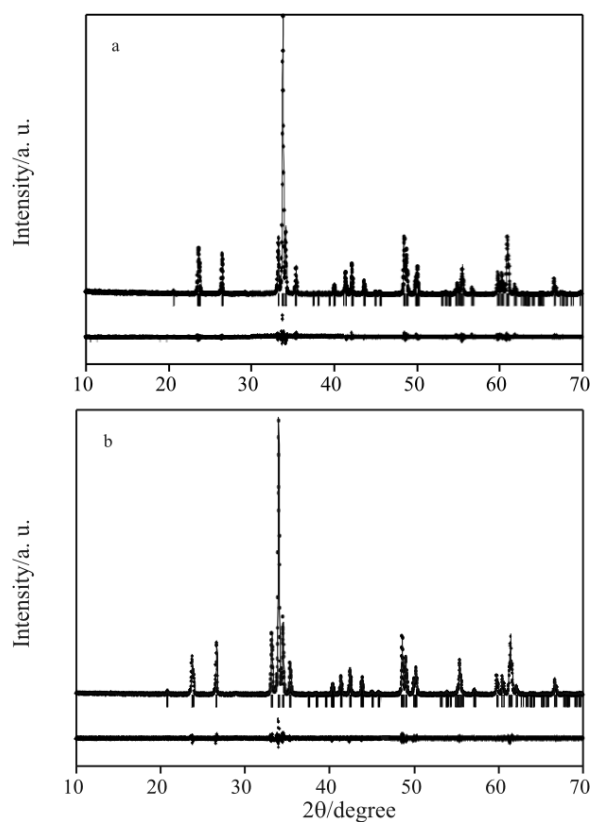


Fig. 10 Rietveld refinement profile of a – $\text{Gd}_{0.5}\text{Eu}_{0.5}\text{CoO}_3$ and b – $\text{Ho}_{0.5}\text{Eu}_{0.5}\text{CoO}_3$. The dotted line is observed X-ray diffraction profile, and the solid line is a calculated one. The bottom curve shows the difference of observed and calculated ones, and the small bars indicate the angular positions of the allowed Bragg refractions

Table 1 Crystallographic data of $\text{Gd}_{0.5}\text{Eu}_{0.5}\text{CoO}_3$ and $\text{Ho}_{0.5}\text{Eu}_{0.5}\text{CoO}_3$

	$\text{Gd}_{0.5}\text{Eu}_{0.5}\text{CoO}_3$	$\text{Ho}_{0.5}\text{Eu}_{0.5}\text{CoO}_3$
Crystal system	orthorhombic	orthorhombic
Space group	<i>Pnma</i>	<i>Pnma</i>
$a/\text{\AA}$	5.38186	5.39667
$b/\text{\AA}$	7.476674	7.422734
$c/\text{\AA}$	5.24183	5.19882
Reliability factor		
$R_{wp}/\%$ ^a	17.31	15.49
$R_p/\%$ ^b	10.88	9.88
$R_e/\%$ ^c	14.835	13.44
$R_I/\%$ ^d	2.44	2.03
$R_F/\%$ ^e	3.26	2.25
S^f	1.1668	1.1344

^a*R*-weighed pattern, ^b*R*-pattern, ^c*R*-expected,

^d*R*-integrated intensity, ^e*R*-structure factor and

^f'Goodness-of-fit' indicator

oxides, $\text{Gd}_{0.5}\text{Eu}_{0.5}\text{CoO}_3$ and $\text{Ho}_{0.5}\text{Eu}_{0.5}\text{CoO}_3$ were orthorhombic and *Pnma*, and the other oxides ($x=0.5$) were also to be similar structure.

The magnetic properties of $\text{Gd}_x\text{Eu}_{1-x}\text{CoO}_3$ ($x=0\sim 1$) and $\text{Ho}_x\text{Eu}_{1-x}\text{CoO}_3$ ($x=0\sim 1$)

Author measured the magnetic susceptibility of EuCoO_3 , $\chi_m(\text{EuCoO}_3)$ in the temperature ranges from 5 to 300 K [7]. The $\chi_m(\text{EuCoO}_3)$ showed a typical Van Vleck magnetic property and Co^{3+} ions of EuCoO_3 were in the low spin ground state ($t_{2g}^6 e_g^0$, $S=0$). The $\chi_m(\text{EuCoO}_3)$ depended on the Eu^{3+} ions was simulated by means of the equation proposed by Van Vleck [7, 15, 16].

The relationships between the magnetic susceptibilities and temperatures for $\text{Gd}_{0.3}\text{Eu}_{0.7}\text{CoO}_3$ and EuCoO_3 were shown in Fig. 11. The temperature dependency of $\chi_m(\text{Gd}_{0.3}\text{Eu}_{0.7}\text{CoO}_3)$ was different from that of EuCoO_3 , and the $\chi_m(\text{Gd}_{0.3}\text{Eu}_{0.7}\text{CoO}_3)$ increased rapidly with decreasing temperature at low temperature. If the Co^{3+} ions were also presumed diamagnetic, the $\chi_m(\text{Gd}_{0.3}\text{Eu}_{0.7}\text{CoO}_3)$ is dependent on the paramagnetic Gd^{3+} ($4f^7$, $L=0$, $S=7/2$ and $J=7/2$) and Eu^{3+} ($4f^6$, $L=3$, $S=3$ and $J=0$) ions. Assuming the additivity of the magnetic susceptibility of component, the $\chi_m(\text{Gd}_{0.3}\text{Eu}_{0.7}\text{CoO}_3)$ was estimated in the temperature ranges from 5 to 300 K using the Van Vleck equation [7, 15], and the values were compatible with those observed ones (Fig. 11). In addition to the $\chi_m(\text{EuCoO}_3)$ and $\chi_m(\text{Gd}_{0.3}\text{Eu}_{0.7}\text{CoO}_3)$, Fig. 11 shows the magnetic susceptibilities of $\text{Gd}_{0.5}\text{Eu}_{0.5}\text{CoO}_3$ and GdCoO_3 . The $\chi_m(\text{Gd}_x\text{Eu}_{1-x}\text{CoO}_3)$ increased with increasing of the value of x .

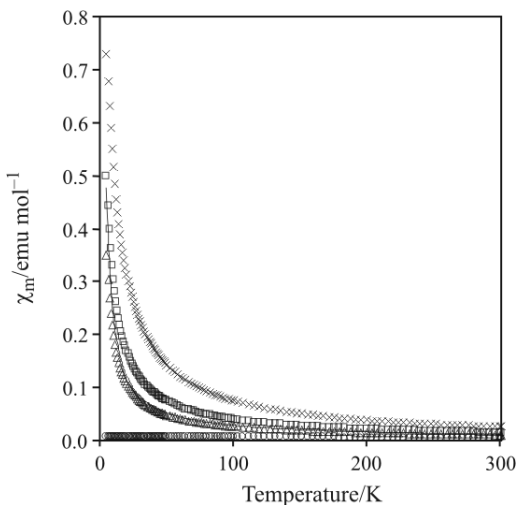


Fig. 11 Magnetic susceptibilities: ○ – observed $\chi_m(\text{EuCoO}_3)$, △ – observed $\chi_m(\text{Gd}_{0.3}\text{Eu}_{0.7}\text{CoO}_3)$, □ – observed $\chi_m(\text{Gd}_{0.3}\text{Eu}_{0.7}\text{CoO}_3)$, × – observed $\chi_m(\text{GdCoO}_3)$, — – estimated $\chi_m(\text{Gd}_{0.3}\text{Eu}_{0.7}\text{CoO}_3)$

The relationships between the magnetic susceptibilities of $\text{Ho}_x\text{Eu}_{1-x}\text{CoO}_3$, $\chi_m(\text{Ho}_x\text{Eu}_{1-x}\text{CoO}_3)$ and temperature showed similar behaviors of those of $\text{Gd}_x\text{Eu}_{1-x}\text{CoO}_3$ described above.

Authors expected novel magnetic properties of $\text{Ln}_x\text{Eu}_{1-x}\text{CoO}_3$ substituted the Eu^{3+} ion with the another lanthanide ion which has different ionic radius of Eu^{3+} ion. However, it seemed to be normal that the magnetic susceptibilities of $\text{Gd}_x\text{Eu}_{1-x}\text{CoO}_3$ and $\text{Ho}_x\text{Eu}_{1-x}\text{CoO}_3$ increased in the temperature dependence with increasing substituted amounts of the species with large J values.

Conclusions

In order to prepare the perovskite-type oxides, $\text{Gd}_x\text{Eu}_{1-x}\text{CoO}_3$ and $\text{Ho}_x\text{Eu}_{1-x}\text{CoO}_3$, the complexes of $\text{Gd}_x\text{Eu}_{1-x}[\text{Co}(\text{CN})_6]\cdot 4\text{H}_2\text{O}$ and $\text{Ho}_x\text{Eu}_{1-x}[\text{Co}(\text{CN})_6]\cdot 4\text{H}_2\text{O}$ were synthesized as the precursors. The crystal structures of $\text{Gd}_x\text{Eu}_{1-x}[\text{Co}(\text{CN})_6]\cdot 4\text{H}_2\text{O}$ and $\text{Ho}_x\text{Eu}_{1-x}[\text{Co}(\text{CN})_6]\cdot 4\text{H}_2\text{O}$ were orthorhombic $Cmcm$, and their lattice parameters were refined by means of the Rietveld method. In the range of $0 \leq x \leq 1$, their lattice parameters decreased linearly with the increased value of x .

The perovskite-type oxides, $\text{Gd}_x\text{Eu}_{1-x}\text{CoO}_3$ and $\text{Ho}_x\text{Eu}_{1-x}\text{CoO}_3$ were obtained by the thermal

decompositions of $\text{Gd}_x\text{Eu}_{1-x}[\text{Co}(\text{CN})_6]\cdot 4\text{H}_2\text{O}$ and $\text{Ho}_x\text{Eu}_{1-x}[\text{Co}(\text{CN})_6]\cdot 4\text{H}_2\text{O}$, respectively. $\text{Gd}_x\text{Eu}_{1-x}\text{CoO}_3$ and $\text{Ho}_x\text{Eu}_{1-x}\text{CoO}_3$ were orthorhombic and $Pnma$. In the ranges of $0 \leq x \leq 1$, their lattice parameters of a -axis linearly lengthen with the increase of the value of x , but those of b - and c -axes decrease with the increase of x .

In the $\text{Gd}_x\text{Eu}_{1-x}\text{CoO}_3$ and $\text{Ho}_x\text{Eu}_{1-x}\text{CoO}_3$, Co^{3+} ions were in the low spin state ($t_{2g}^6 e_g^0$, $S=0$), therefore their magnetic susceptibilities were dependent on the component of the Eu^{3+} , Gd^{3+} and Ho^{3+} ions in the temperature ranges from 5 to 300 K. The magnetic susceptibilities of $\text{Gd}_x\text{Eu}_{1-x}\text{CoO}_3$ and $\text{Ho}_x\text{Eu}_{1-x}\text{CoO}_3$ increased in the temperature dependence with increasing substituted amounts of the species with large J values.

References

- 1 S. E. Dann, D. B. Currie and M. T. Weller, J. Solid State Chem., 109 (1994) 134.
- 2 K. Yoshii, J. Solid State Chem., 159 (2001) 204.
- 3 P. K. Gallagher, Mater. Res. Bull., 3 (1968) 225.
- 4 Y. Masuda, K. Nagaoka, H. Ogawa, O. Nakazato, Y. Yukawa and H. Miyamoto, J. Alloys Compd., 235 (1996) 23.
- 5 W. Xiaoyu, Y. Yukawa and Y. Masuda, J. Alloys Compd., 290 (1999) 85.
- 6 K. Asai, A. Yoneda, O. Yokokura, J. M. Tranquada, G. Shirane and K. Kohn, J. Phys. Soc. Jpn., 67 (1998) 290.
- 7 K. Umemoto, Y. Seto and Y. Masuda, Thermochim. Acta, 431 (2005) 117.
- 8 F. Izumi and T. Ikeda, Mater. Sci. Forum, 198 (2000) 321.
- 9 Y. Masuda, K. Kikuchi, Y. Yukawa and H. Miyamoto, J. Alloys Compd., 260 (1997) 70.
- 10 Y. Masuda, Y. Seto, X. Wang, Y. Yukawa and T. Arii, J. Therm. Anal. Cal., 60 (2000) 1033.
- 11 Y. Masuda, Y. Seto, X. Wang and Y. Tuchiya, J. Therm. Anal. Cal., 64 (2001) 1045.
- 12 Y. Seto, S. Nagao, X. Wang and Y. Masuda, J. Therm. Anal. Cal., 73 (2003) 755.
- 13 Y. Yukawa, S. Igarashi, T. Kawaura and H. Miyamoto, Inorg. Chem., 35 (1996) 7399.
- 14 Powder Diffraction File, Inorganic Volume, No. 25–1054 (1984).
- 15 J. H. Van Vleck, The Theory of Electric and Magnetic Susceptibilities, Oxford University Press, Oxford 1932.
- 16 L. Sudheendra, Md. M. Seikh, A. R. Raju and C. Narayana, Chem. Phys. Lett., 340 (2001) 275.

DOI: 10.1007/s10973-007-8962-2